

Origin of background electron concentration in $\text{In}_x\text{Ga}_{1-x}\text{N}$ alloys

B. N. Pantha,¹ H. Wang,^{1,*} N. Khan,^{1,2} J. Y. Lin,¹ and H. X. Jiang^{1,†}

¹Department of Electrical & Computer Engineering, Texas Tech University, Lubbock, Texas 79409

²School of Science and Technology, Georgia Gwinnett College, Lawrenceville, GA, 30043

(Received 19 May 2011; published 15 August 2011)

The origin of high background electron concentration (n) in $\text{In}_x\text{Ga}_{1-x}\text{N}$ alloys has been investigated. A shallow donor was identified as having an energy level (E_{D1}) that decreases with x ($E_{D1} = 16$ meV at $x = 0$ and $E_{D1} = 0$ eV at $x \sim 0.5$) and that crossover the conduction band at $x \sim 0.5$. This shallow donor is believed to be the most probable cause of high n in InGaN. This understanding is consistent with the fact that n increases sharply with an increase in x and becomes constant for $x > 0.5$. A continuous reduction in n was obtained by increasing the V/III ratio during the epilayer growth, suggesting that nitrogen vacancy-related impurities are a potential cause of the shallow donors and high background electron concentration in InGaN.

DOI: 10.1103/PhysRevB.84.075327

PACS number(s): 71.20.Nr, 71.55.Eq, 73.61.Ey, 74.25.F–

I. INTRODUCTION

InGaN alloys are used as active media in today's most efficient solid-state lighting devices such as blue/green/white light-emitting diodes and laser diodes.¹ Recent determination of the InN bandgap (0.65 eV)^{2–4} has further broadened the applications of InGaN ternary alloys into areas such as long-wavelength emitters, photovoltaics, and solar-water splitting,^{2–9} made possible by their ability to tune direct bandgap in the entire solar spectrum. InGaN alloys have also attracted considerable attention for their potential applications in thermoelectric power generation at high temperatures.^{10,11} The ability to synthesize high-quality single phase as well as *p*-type alloys is essential for realizing new, high efficiency devices. In an effort to overcome these challenges, synthesizing single-phase InGaN alloys in the middle composition range ($0.25 \leq x \leq 0.63$) and *p*-type InGaN with relatively high In-contents (up to 0.35) have been attempted and partially successful.^{12,13} Nonetheless, there remain considerable difficulties for growing *p*-type $\text{In}_x\text{Ga}_{1-x}\text{N}$ alloys with $x \geq 0.35$. The major obstacle for realizing *p*-type InGaN with relatively high In-contents is the presence of high background electron concentration (n).

Impurities such as H^{14–20} and O^{16,20} nitrogen vacancies (V_N) associated with dislocations,^{21,22} and In vacancy/N antisite ($V_{\text{In}}-N_{\text{In}}$) complexes²³ have been proposed as possible sources of the unintentional donors responsible for high background electron concentration in InN. Since all InN and In-rich $\text{In}_x\text{Ga}_{1-x}\text{N}$ alloys grown by metal organic chemical vapor deposition (MOCVD) possess high n ($\sim 10^{19} \text{ cm}^{-3}$), it is difficult to observe dependence on the growth or postgrowth processing parameters and thus difficult to understand the cause of high n in InGaN. We report here a systematic study of the behavior of the background electron concentration in InGaN alloys synthesized by MOCVD in the whole composition range and attempt to pinpoint a possible origin of high n .

II. EXPERIMENT

$\text{In}_x\text{Ga}_{1-x}\text{N}$ alloys of thickness ~ 180 – 300 nm and GaN epilayers ($x = 0$) of thickness $\sim 1 \mu\text{m}$ were grown directly on AlN/sapphire templates by MOCVD. The precursors were trimethylgallium (TEG), trimethylindium (TMI), and ammo-

nia (NH_3) for Ga, In, and N, respectively. The growth pressure was in the range of 300 to 600 torr. Growth temperature was varied from 1050 to 570 °C as x was increased from 0 to 1. The variation of V/III ratio was obtained in the following two ways: V/III ratio can be increased by reducing molar flow of group III-precursor or by increasing molar flow of group V precursor. In-contents were determined from the peak angles of (002) θ - 2θ x-ray diffraction (XRD) curves based on Vegard's law. Selective samples were also examined by secondary ion mass spectrometry (SIMS) measurement to confirm the In-contents in InGaN epilayers. For Hall-effect measurements, we prepared ohmic contacts [Ti (30 nm)/Al (100 nm)/Ni (30 nm)/Au (120 nm)] on samples by e-beam evaporation.

III. RESULTS AND DISCUSSION

Figure 1 shows XRD θ - 2θ scan curves of the (002) reflection peaks in $\text{In}_x\text{Ga}_{1-x}\text{N}$ alloys. The peak position of XRD θ - 2θ curves continuously shifts toward the lower angles with respect to GaN and reaches the InN position. This implies that these InGaN films are of single phase and that the theoretically predicted miscibility gap²⁴ can be breached. The reasons for phase-separation suppression have previously been addressed.^{12,25,26} The full-width at half maximum (FWHM) of XRD (002) rocking curves of $\text{In}_x\text{Ga}_{1-x}\text{N}$ as a function of x is plotted in Fig. 2(a). FWHM increased from 300 arcsec for pure GaN ($x = 0$) to about 4000 arcsec for x between 0.5 and 0.8, and then decreased to 1000 arcsec for pure InN ($x = 1$). The solid line is the Gaussian fit of the data with a peak at $x \sim 0.6$. These results clearly indicate that the crystalline quality of $\text{In}_x\text{Ga}_{1-x}\text{N}$ in the middle composition range is inferior to that of either end.

Broadening of XRD rocking curves is mainly caused by threading dislocations (TDs), which are generated due to a large lattice mismatch of epitaxial film to the substrate. During the growth of InGaN alloys on AlN templates, lattice constant of InGaN alloys increases linearly as In content increases and hence a linear increase in FWHM of rocking curve is expected. In contrast we observed a nonlinear behavior of FWHM of XRD rocking curves with In content in InGaN alloys with peak around In content = 0.6. The exact reason for much broader rocking curves in the middle In composition is not fully understood, however some possible reasons could be:

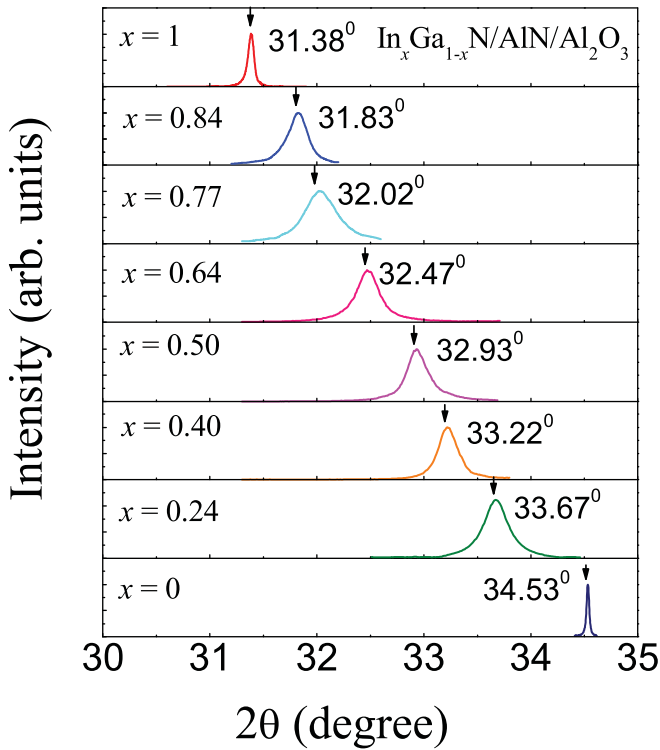


FIG. 1. (Color online) (002) XRD θ - 2θ curves of $\text{In}_x\text{Ga}_{1-x}\text{N}$ alloys. Single narrow peaks for all compositions indicate that there is no-phase separation.

(1) there might still be some degree of microscopic-phase separation which limits the coherency of diffracted x-rays, (2) large internal strain caused by a large difference in atomic size of GaN and InN as rocking curves can be broadened due to strain,²⁷ (3) growth conditions of InGaN alloys in the middle range are not as matured as those of In-rich and Ga-rich region, and (4) high concentrations of impurities and vacancies.

In Fig. 2(b) and 2(c), we plotted the room-temperature electron mobility μ and concentration n of $\text{In}_x\text{Ga}_{1-x}\text{N}$ as functions of x . Standard scattering mechanisms in InGaN alloys are alloy disorder, acoustic/optical phonons, impurities, and dislocations. The total mobility is $\mu_{\text{Tot}}^{-1} = \mu_{al}^{-1} + \mu_V^{-1}$, where μ_{al} is the contribution from alloy scattering and μ_V is related to acoustic/optical phonon, impurity, and dislocation scatterings. Since random alloys in a crystal introduce short-range potential, the alloy-scattering limited-electron mobility μ_{al} can be described by the following equation²⁸:

$$\mu_{al}(x) = \frac{(2\pi)^{1/2}e\hbar^4}{3(kT)^{1/2}\Omega(m_e)^{5/2}x(1-x)(\Delta U_e)^2} \quad (1)$$

where m_e is the electron-effective mass, Ω is volume of primitive cell, $\Delta U_e = |V_A - V_B|$ is the difference in potential between the two binaries (or alloy scattering potential), and x is alloy-mole fraction. We have chosen $m_e = 0.133m_o$ [a mean electron-effective mass of InN ($m_e = 0.047m_o$) and GaN ($m_e = 0.22m_o$)], $\Omega = 2.283 \times 10^{-23} \text{ cm}^{-3}$ (volume of primitive cell of GaN) and ΔU_e as fitting parameter. All numerical values were taken from Ref. 28. Fitting of experimental data with Eq. (1), except at two end points ($x = 0$, GaN and $x = 1$, InN), yields

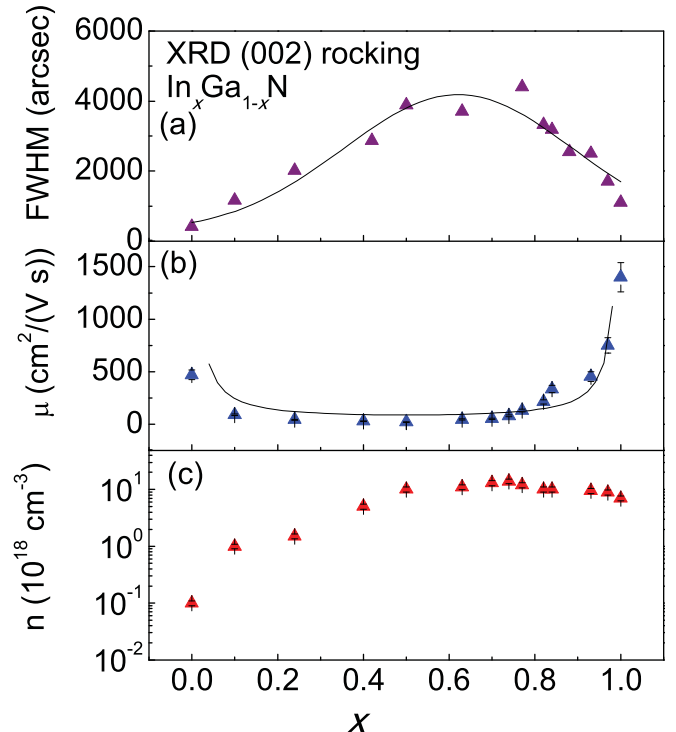


FIG. 2. (Color online) (a) FWHM of (002) XRD rocking curves. Solid line was obtained by fitting data to Gaussian distribution. (b) Room-temperature electron mobility μ measured by Hall effect experiments. Solid line shows the least-squares fit using Eq. (1). (c) Room-temperature free electron concentration n obtained by Hall effect experiment.

$\Delta U_e = 6.1$ eV. The alloy-scattering limited-electron mobility μ_{al} as a function of x with different ΔU_e in $\text{In}_x\text{Ga}_{1-x}\text{N}$ alloys is calculated according to Ridley's model outlined in Ref. 28. The minimum calculated value of μ_{al} was $400 \text{ cm}^2/\text{Vs}$ for $\Delta U_e = 2.1$ eV. This value of μ_{al} is much higher than our experimental value because of the smaller ΔU_e since μ_{al} is quadratically inversely proportional to this potential. The deviation of our data from this model could be because of scattering of electrons by dislocations and impurities. Since the term $x(x-1)$ is maximized at $x = 0.5$, one would expect a minimum value of μ_{al} at this composition, which is consistent with our results.

In Fig. 2(c) we plotted n as a function of x , which increased by two orders of magnitude from $\sim 10^{17} \text{ cm}^{-3}$ for GaN ($x = 0$) to $\sim 10^{19} \text{ cm}^{-3}$ for $\text{In}_{0.5}\text{Ga}_{0.5}\text{N}$ and remained almost constant thereafter. Such a high value of n ($\sim 10^{19} \text{ cm}^{-3}$) in InN and In-rich InGaN has been repeatedly observed by many groups^{15–23,29}; however, the behavior of n in the entire alloy range has not been reported. To understand the origin of high background electron concentration, we have measured the temperature dependent n in $\text{In}_x\text{Ga}_{1-x}\text{N}$ alloys ($0 \leq x \leq 0.4$). Variations of n with the reciprocal temperature $1/T$ for $x = 0, 0.1, 0.24$, and 0.4 are shown in Fig. 3(a). Solid lines result from a least-squares fit of data by using the following simplified formula of two impurity level conduction (except for GaN),

$$n = N_{D1} \exp\left(\frac{-E_{D1}}{k_B T}\right) + N_{D2} \exp\left(\frac{-E_{D2}}{k_B T}\right), \quad (2)$$

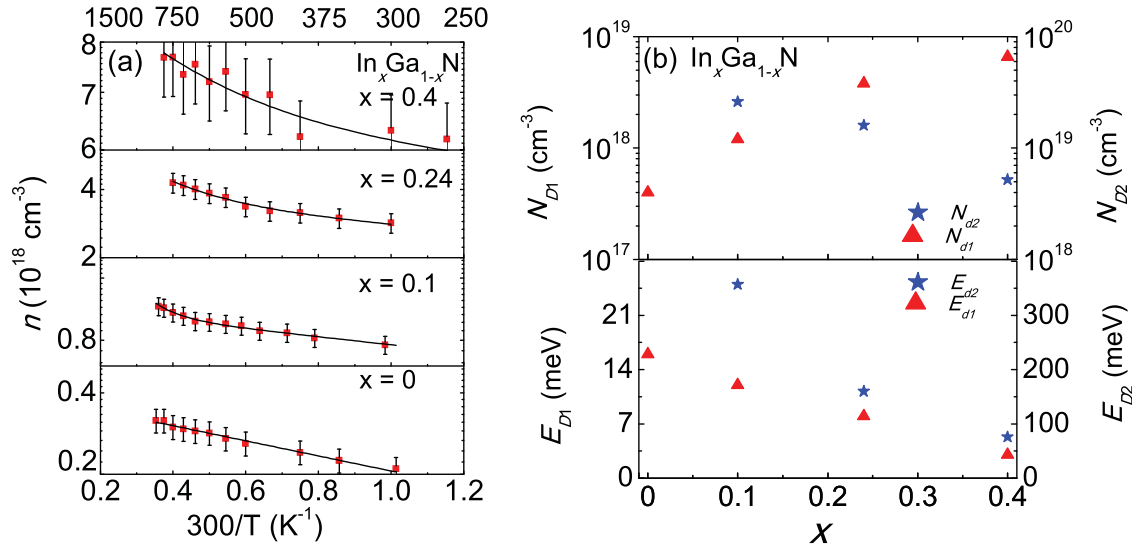


FIG. 3. (Color online) (a) Arrhenius plot of electron concentration n for $\text{In}_x\text{Ga}_{1-x}\text{N}$ ($0 \leq x \leq 0.4$) alloys. The solid lines result from a least-squares fit of data by Eq. (2). (b) Donor concentrations and corresponding energy levels as functions of In content, x .

where N_{D1} and N_{D2} are donor concentrations with energy levels E_{D1} and E_{D2} , respectively. The data fit well with Eq. (2), indicating that two donor levels exist in InGaN alloys.

In Fig. 3(b) we plotted the fitting results, i.e., concentrations and energy levels of these two donor impurities, as functions of x . Energy levels of both donors were found to decrease with increasing x . The shallower donor concentration N_{D1} increased while the deeper donor concentration N_{D2} decreased with increasing x . In an undoped GaN, we found only the shallow donor with an energy level (E_{D1}) of about 16 meV at a concentration of $\sim 10^{17} \text{ cm}^{-3}$. A deep level, $E_{D2} \sim 360$ meV below the conduction band emerged in $\text{In}_{0.1}\text{Ga}_{0.9}\text{N}$, and its energy level decreased with increasing x . In $\text{In}_x\text{Ga}_{1-x}\text{N}$ alloys with high x , the dominating donor impurity responsible for high n is apparently the shallow one. For instance, at $x = 0.4$, the shallow level with $N_{D1} \sim 6 \times 10^{18} \text{ cm}^{-3}$ ($E_{D1} \sim 3$ meV) and deep level with $N_{D2} \sim 4 \times 10^{18} \text{ cm}^{-3}$ ($E_{D2} \sim 70$ meV) will contribute $\sim 5.5 \times 10^{18} \text{ cm}^{-3}$ and $\sim 2 \times 10^{17} \text{ cm}^{-3}$, respectively, to the background electron concentration at room temperature. It is clear that the contribution of N_{D2} to n is further decreased and is much smaller than the contribution of N_{D1} at $x > 0.5$, assuming the number of shallow donors remains about the same in In-rich InGaN alloys.

On the basis of Fig. 3(b) a schematic band diagram of $\text{In}_x\text{Ga}_{1-x}\text{N}$ including this shallow donor level is constructed in Fig. 4. It was found that E_{D1} is positioned as close as 3 meV below the conduction band at $x = 0.4$. The results clearly indicate that E_{D1} will crossover the conduction band at $x \sim 0.5$. In this situation we expect that all shallower donors are thermally excited at room temperature, providing the maximum possible n . This observation explains the n vs x plot of Fig. 2(c) which shows that n reached its maximum value at $x \sim 0.5$ and remained constant thereafter. High n in the middle composition range is most likely related to the deficiency of active nitrogen atoms as InGaN alloys in this region were grown at high growth rate and/or low V/III ratio to avoid phase separation. Deficiency of active nitrogen atoms can generate nitrogen vacancy related

impurities. Effect of V/III ratio on n is to be described later.

Figure 5(a) shows the SIMS measurement results of $\text{In}_{0.24}\text{Ga}_{0.76}\text{N}$ alloys grown at two different V/III ratios (8400 and 19600). SIMS results show that concentrations of all investigated elements, H, O, Si, and C, are very high (on the order of 10^{19} cm^{-3} or even higher at a depth of ~ 50 nm). The unusually high concentration of H and O near the surface could be due to the postgrowth surface contamination and artificial effects from SIMS measurements. Although H concentration in as-grown GaN can be as high as $10^{18}\text{--}10^{19} \text{ cm}^{-3}$,¹ the

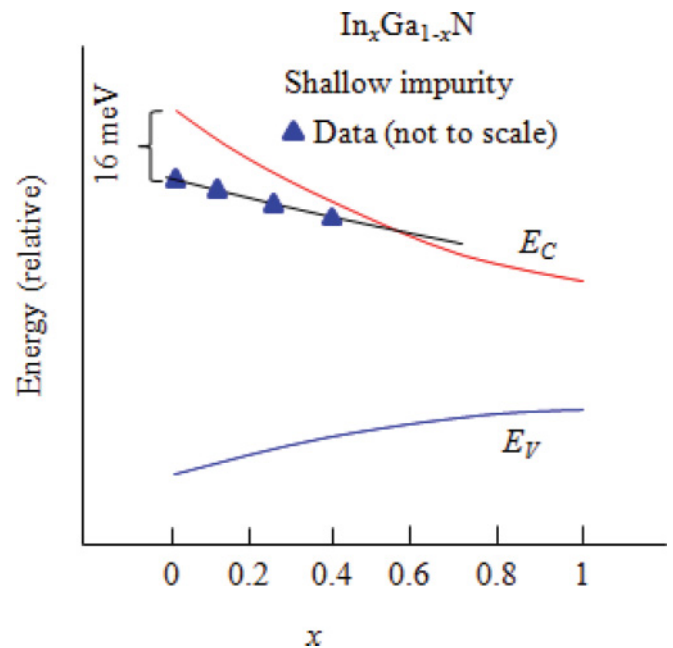


FIG. 4. (Color online) The shallow donor level with respect to the conduction band edge as a function of In content, x . The shallow donor energy level (E_{D1}) is expected to crossover the conduction band around $x = 0.5$.

main donors in GaN have been attributed to Si^{30,31} and O.³¹ In the case of InN both calculations and experiments indicated that *H* impurities, both interstitial (H_i) and substitutional (H_N), are the most probable candidates for high n ^{15–21} and may be partially diffused out by postgrowth thermal annealing.^{19,20,32,33}

Figure 5(b) shows the concentrations of these unintentionally doped impurities in the films at a depth of 100 nm, obtained from SIMS measurements. The results show that the concentration of Si in both films is less than the measured values of n ; therefore, the possibility of Si impurity as a source of the background electrons can be excluded. On the other hand the concentration of O is much higher ($1.1 \times 10^{19} \text{ cm}^{-3}$ and $3.6 \times 10^{18} \text{ cm}^{-3}$ for films with V/III ratio = 8400 and 19600, respectively) than the measured n ($2.8 \times 10^{18} \text{ cm}^{-3}$ and $2.0 \times 10^{18} \text{ cm}^{-3}$ for the films with V/III ratio = 8400 and 19600, respectively). Moreover, the decrease in O impurity concentration with increasing V/III ratio is not consistent with the decrease in the background electron concentration with increasing V/III ratio ($3 \times$ vs $1.4 \times$). This implies that O impurity is not necessarily a source of n either.

In the middle In composition range FWHMs of (002) rocking curves of InGaN alloys are found to be much larger than those in the either side. The corresponding total density of TDs in these InGaN alloys may be in the range of 10^{11} cm^{-2} if we consider the fact that in-plane rocking curves are even broader than (002) rocking curves. It is a well-established fact that TDs can reduce electron mobility as they act as scattering centers for electrons but they may not contain such a high density of n , as we observed here in the middle In composition range InGaN alloys. Our previous results show that n remains almost the same in $\text{In}_{0.65}\text{Ga}_{0.35}\text{N}$ alloys over the wide range of FWHMs of (002) rocking curves, while the electron mobility is found to increase as FWHM of rocking curves decreases.²⁶ Additionally, a recent study in In-face InN by Gallinat *et al.*¹⁸ suggested that TDs act only as scattering centers which limit the electron mobility. More importantly high density of dislocations should not introduce a shallow donor level.

Other possible shallow donor candidates include nitrogen vacancies (V_N).^{33,34} The contribution of V_N to the background electron concentration in GaN is expected to be low due to the high-formation energy of V_N in GaN. However, nitrogen vacancies are the most probable cause of a residue-electron concentration on the order of 10^{17} cm^3 in a typical good quality, unintentionally doped GaN, due to the low cracking efficiency of NH_3 at 1050°C and thus deficiency of N atoms during MOCVD growth. In contrast the deficiency of N atom is much more severe in InGaN alloys than in GaN due to lower cracking efficiency of NH_3 at reduced growth temperatures (the growth temperature decreases from 1050°C for GaN to $\sim 600^\circ\text{C}$ for In-rich InGaN alloys). This N deficiency significantly increases the concentration of V_N .

To understand the severity of nitrogen deficiencies, we have monitored n for $\text{In}_{0.24}\text{Ga}_{0.76}\text{N}$ alloys grown with varying V/III ratios and found that the values of n decrease with increasing V/III ratio, as shown in Fig. 5(c). A higher V/III ratio should provide more active nitrogen atoms during growth

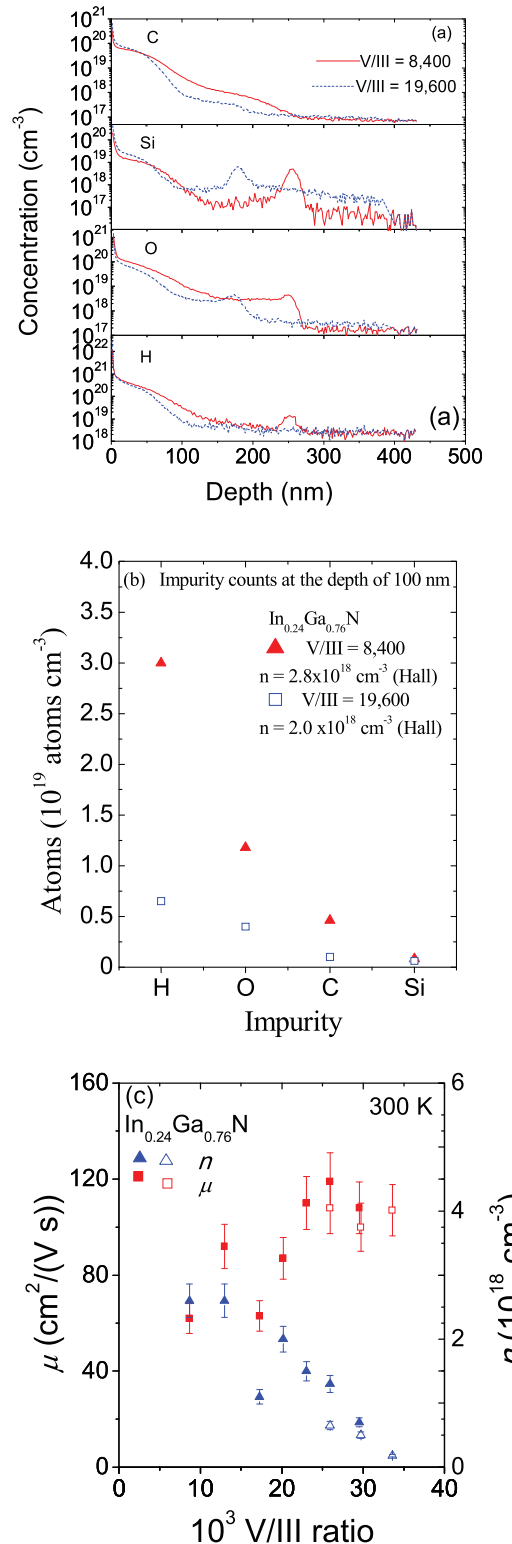
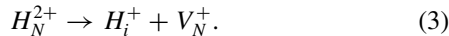


FIG. 5. (Color online) (a) SIMS profiles of H, O, Si, and C impurities (performed by Evan Analytical Group). (b) Concentrations of H, O, Si, and C impurities at a depth of 100 nm of $\text{In}_{0.24}\text{Ga}_{0.76}\text{N}$ samples grown with two different V/III ratios of 8400 and 19600. (c) μ and n as functions of V/III ratio. Open (closed) symbol data are obtained by reducing (increasing) trimethylgallium (ammonia) molar flow in gas phase.

and compensate for the deficiency of N atoms, which in turn reduces the concentration of V_N and/or H_N . The overall material quality also improved with increasing V/III ratio as evidenced by a linear increase in electron mobility with an increase in the V/III ratio. These results seem to suggest that in addition to interstitial H_i , V_N , and/or H_N are also major donors in InGaN, particularly in In-rich InGaN alloys.

It has been shown that the background electron concentration can be reduced via out-diffusion of H by thermal annealing. However, n values in such annealed samples remain very high, implying the possibility of other donors. Based on our results, we suggest that singly charged V_N -related impurities are one of the major causes of residual n in InGaN. In such a context the main donors in InN or In-rich InGaN alloys are H^{14} and V_N -related impurities. A recent calculation suggested that in addition to interstitial H_i^+ , substitution H_N^{2+} is also a potential cause of high n in InN. It was discussed that H_N^{2+} can migrate via three distinct processes. Among them, the dissociation process (as described by the following equation) has the lowest activation energy,



If we assume concentrations of H_N^{2+} , H_i^+ , and V_N^+ in an as-grown InN or In-rich InGaN are the same, from the previous reaction we have $N[H_N^{2+}] = N[H_i^+] = N[V_N^+]$, while annealing can only reduce n by half via out-diffusion of H_i^+ (*in situ* incorporated H_i^+ and H_i^+ formed by dissociation process of H_N^{2+} during annealing). V_N^+ cannot be diffused out and is thus responsible for residual n in annealed materials. This reduction

of background n by half has been observed in InN grown under different growth conditions by several groups^{19,20,32} and validates our previous discussion. The reduction factor depends upon the ratio of H to V_N concentrations. This explains the fact that a reduction in background n by more than half has also been observed.³³

IV. CONCLUSION

In summary we have investigated the origin of the background electron concentration in $In_xGa_{1-x}N$. It was observed that the background electron concentration increases sharply with an increase in x for $x < 0.5$ and became almost constant ($n \sim 10^{19} \text{ cm}^{-3}$) for $x > 0.5$. Our results suggest that the formation of nitrogen vacancy (V_N) related impurities due to an insufficient supply of N atoms at reduced growth temperatures ($\sim 600^\circ\text{C}$) is primarily responsible for the high background electron concentration in In-rich InGaN alloys. This V_N -related donor is very shallow. Its energy level decreases with an increase in In content and crossover the conduction band at $x \sim 0.5$. Unlike hydrogen impurities, V_N -related impurities in InN and In-rich InGaN alloys cannot be annealed out.

ACKNOWLEDGMENTS

The work was supported by DOE (Grant No. DE-FG 03-96ER45604). Lin and Jiang gratefully acknowledge the support of the Linda Whitacre and Ed Whitacre endowed chair positions through the AT&T Foundation.

*Present address: InvenLux Corporation, 9650 Telstar Ave., El Monte, CA 91731.

[†]Corresponding author: hx.jiang@ttu.edu

¹S. Nakamura and G. Fasol, *The Blue Laser Diode* (Springer, Berlin, 1997).

²J. Wu, W. Walukiewicz, K. M. Yu, J. W. Ager, E. E. Haller, H. Lu, and W. J. Schaff, *Appl. Phys. Lett.* **80**, 4741 (2002).

³J. Wu, W. Walukiewicz, K. M. Yu, J. W. Ager III, E. E. Haller, H. Lu, W. J. Schaff, Y. Saito, and Y. Nanishi, *Appl. Phys. Lett.* **80**, 3967 (2002).

⁴V. Yu. Davydov, A. A. Klochikhin, R. P. Seisyan, V. V. Emtsev, S. V. Ivanov, F. Bechstedt, J. Furthmüller, H. Harima, A. V. Mudryi, J. Aderhold, O. Semchinova, and J. Graul, *Phys. Status Solidi B* **229**, R1 (2002).

⁵R. Dahal, B. Pantha, J. Li, J. Y. Lin, and H. X. Jiang, *Appl. Phys. Lett.* **94**, 063505 (2009).

⁶O. Jani, I. Ferguson, C. Honsberg, and S. Kurtz, *Appl. Phys. Lett.* **91**, 132117 (2007).

⁷C. J. Neufeld, N. G. Toledo, S. C. Cruz, M. Iza, S. P. DenBaars, and U. K. Mishra, *Appl. Phys. Lett.* **93**, 143502 (2008).

⁸R. Dahal, B. Pantha, J. Li, J. Y. Lin, and H. X. Jiang, *Appl. Phys. Lett.* **94**, 063505 (2009).

⁹J. Li, J. Y. Lin, and H. X. Jiang, *Appl. Phys. Lett.* **93**, 162107 (2008).

¹⁰B. N. Pantha, R. Dahal, J. Li, J. Y. Lin, H. X. Jiang, and G. Pomrenke, *Appl. Phys. Lett.* **92**, 042112 (2008).

¹¹A. Sztein, H. Ohta, J. Sonoda, A. Ramu, J. E. Bowers, S. P. DenBaars, and S. Nakamura, *Appl. Phys. Exp.* **2**, 111003 (2009).

¹²B. N. Pantha, J. Li, J. Y. Lin, and H. X. Jiang, *Appl. Phys. Lett.* **93**, 182107 (2008).

¹³B. N. Pantha, A. Sedhain, J. Li, J. Y. Lin, and H. X. Jiang, *Appl. Phys. Lett.* **95**, 261904 (2009).

¹⁴A. Janotti and C. G. Van de Walle, *Appl. Phys. Lett.* **92**, 032104 (2008).

¹⁵D. C. Look, H. Lu, W. Schaff, J. Jasinski, and Z. Liliental-Weber, *Appl. Phys. Lett.* **80**, 258 (2002).

¹⁶C. S. Gallinat, G. Koblmüller, J. S. Brown, S. Bernardis, J. S. Speck, G. D. Chern, E. D. Readinger, H. Shen, and M. Wraback, *Appl. Phys. Lett.* **89**, 032109 (2006).

¹⁷V. Darakchieva, T. Hofmann, M. Schubert, B. E. Sernelius, B. Monemar, P. O. Å. Persson, F. Giuliani, E. Alves, H. Lu, and W. J. Schaff, *Appl. Phys. Lett.* **94**, 022109 (2009).

¹⁸C. S. Gallinat, G. Koblmüller, and J. S. Speck, *Appl. Phys. Lett.* **95**, 022103 (2009).

¹⁹V. Darakchieva, K. Lorenz, N. P. Barradas, E. Alves, B. Monemar, M. Schubert, N. Franco, C. L. Hsiao, L. C. Chen, W. J. Schaff, L. W. Tu, T. Yamaguchi, and Y. Nanishi, *Appl. Phys. Lett.* **96**, 081907 (2010).

- ²⁰S. Ruffenach, M. Moret, O. Briot, and B. Gil, *Appl. Phys. Lett.* **95**, 042102 (2009).
- ²¹V. Cimalla, V. Lebedev, F. M. Morales, R. Goldhahn, and O. Ambacher, *Appl. Phys. Lett.* **89**, 172109 (2006).
- ²²L. F. J. Piper, T. D. Veal, C. F. McConville, H. Lu, and W. J. Schaff, *Appl. Phys. Lett.* **88**, 252109 (2006).
- ²³K. S. A. Butcher, A. J. Fernandes, P. P.-T. Chen, M. Winterbert-Fouquet, H. Timmers, S. K. Shrestha, H. Hirshy, R. M. Perks, and B. F. Usher, *J. Appl. Phys.* **101**, 123702 (2007).
- ²⁴I. Ho and G. B. Stringfellow, *Appl. Phys. Lett.* **69**, 2701 (1996).
- ²⁵S. Y. Karpov, MRS Internet J. Nitride Semicond. Res. **3**, 16 (1998).
- ²⁶B. N. Pantha, A. Sedhain, J. Li, J. Y. Lin, and H. X. Jiang, *Appl. Phys. Lett.* **96**, 232105 (2010).
- ²⁷J. E. Ayers, *J. Cryst. Growth* **135**, 71 (1994).
- ²⁸H. Morkoc, *Hand Book of Nitride Semiconductor and Device*, Vol. 2 (Wiley-VCH, Verlag GmBh &Co. KGaA, Weinheim, 2008), p. 212–218.
- ²⁹N. Khan, A. Sedhain, J. Li, J. Y. Lin, and H. X. Jiang, *Appl. Phys. Lett.* **92**, 172101 (2008).
- ³⁰W. Götz, N. M. Johnson, D. P. Bour, C. Chen, H. Liu, C. Kuo, and W. Imler, *Mater. Res. Soc. Symp. Proc.* **395**, 443 (1996).
- ³¹W. J. Moore, J. A. Freitas Jr., G. C. B. Braga, R. J. Molnar, S. K. Lee, K. Y. Lee, and I. J. Song, *Appl. Phys. Lett.* **79**, 2570 (2001).
- ³²G. Pettinari, F. Masia, M. Capizzi, A. Polimeni, M. Losurdo, G. Bruno, T. H. Kim, S. Choi, A. Brown, V. Lebedev, V. Cimalla, and O. Ambacher, *Phys. Rev. B* **77**, 125207 (2008).
- ³³W. Huang, M. Yshimoto, K. Harima, and J. Saraie, *Jpn. J. Appl. Phys.* **43**, L97 (2004).
- ³⁴Q. Yang, H. Feick, and E. R. Weber, *Appl. Phys. Lett.* **82**, 3002 (2003).
- ³⁵D. C. Look, D. C. Reynolds, J. W. Hemsky, J. R. Sizelove, R. L. Jones, and R. J. Molnar, *Phys. Rev. Lett.* **79**, 2273 (1997).